I. Green
I. Etsion

Department of Mechanical Engineering,
Technion, Haifa, Israel

Fluid Film Dynamic Coefficients in Mechanical Face Seals

The stiffness and damping coefficients of the fluid film in mechanical face seals are calculated for the three major degrees of freedom of the primary seal ring. The calculation is based on small perturbation of the ring from its equilibrium position. Analytical expressions are presented for the various coefficients and a comparison is made with results of accurate but more complex analyses to establish the range of applicability.

Introduction

A mechanical face seal, Fig. 1, is basically a dynamic system in which a flexibly mounted primary seal ring is separated by a thin fluid film from a rotating seat. The ability of the flexibly mounted ring to track the rotating seat in a controlled manner is of great importance for safe operation of the seal. The subject of mechanical face seal dynamics is attracting a growing amount of interest recently, [1] to [9], and as the demand for higher operating speeds in rotating machines increases the importance of seal dynamics becomes more and more evident.

Problems related to vibrations in mechanical face seals have been documented in the literature since the early 60's [10] to [12]. However, due to its complexity, theoretical treatment of the problem has been very limited in scope. Examples can be found in references [13] to [16] from the mid 70's. A common drawback in all of these works is the lack of accurate information on the dynamic properties of the thin fluid film, which consequently leads to crude approximations. Even in more recent works e.g. [2] and [6] the stiffness and damping coefficients of the fluid film are only estimated or generally postulated. Since the fluid film is a major component of the seal system, its dynamic properties must be known if a comprehensive dynamic analysis is to be performed. It is the aim of this work, therefore, to calculate the dynamic coefficients of the fluid film in a mechanical face seal and to present them in an orderly fashion. This, it is hoped, will be helpful to seal investigators and result in better seal designs.

Generally, the fluid film dynamic coefficients are nonlinear, however, a good insight into the dynamic behavior of a seal system can be obtained from a linearized solution based on small perturbation. Hence, only the coefficients that are relevant to small perturbation analysis will be considered in this paper.

Theoretical Background

A theoretical model of the mechanical face seal is shown in Fig. 2. The seat rotates at a constant angular velocity, ω, about the axis z of an inertial reference xyz. The primary seal ring can move axially along axis z and can tilt simultaneously about the x and y axes. It is easier to analyze the dynamic coefficients by introducing a rotating coordinate system 123 which coincides with the principal axes of the ring. The system 123 precesses in the inertial reference xyz so that axis 1 always remains in the plane xy and axis 2 is directed to the instantaneous point of maximum film thickness. Thus, the orientation of the coordinate system 123, and the ring, in the inertial reference xyz can be defined by the nutation angle γ^* measured from axis z to axis 3, and by the precession angle ψ^* measured from axis x to axis 1.

The dynamic behavior of the seal ring can be analyzed by solving its equations of motion which have the general form

$$m_j^* \ddot{X}_j^* = \Sigma F_j^* \qquad (1)$$

In equation (1) m_j^*, $\ddot{x}_j^*$, and F_j^* represent generalized mass, acceleration, and force, respectively, in degree of freedom j. The sum of generalized forces, ΣF_j^*, in (1) is combined of both the fluid film and the flexible support contributions. In the following only the fluid film contribution will be considered.

Introducing dynamic coefficients, the sum of generalized forces can be expressed in the form

$$\Sigma F^*{}_j = -\sum_i K_{ij}^* X_i^* - \sum_i D_{ij}^* \dot{X}_i^* \qquad (2)$$

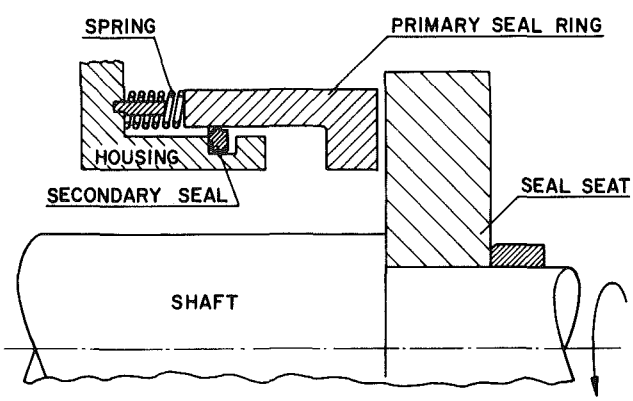

Fig. 1 Schematic of a radial face seal

Contributed by the Lubrication Division of THE AMERICAN SOCIETY OF MECHANICAL ENGINEERS and presented at the ASME/ASLE Joint Lubrication Conference, Washington, D.C., October 5–7, 1982. Manuscript received by the Lubrication Division, February 1, 1982. Paper No. 82-Lub-34.

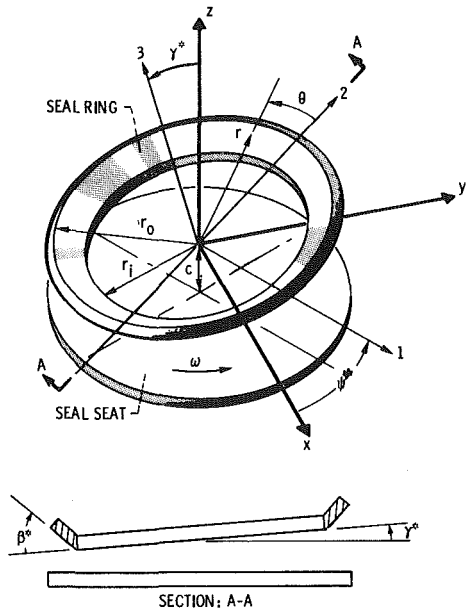

Fig. 2 Seal model and coordinates systems

In (2) K_{ij}^*, and D_{ij}^* are fluid film stiffness and damping coefficients, respectively, generating a response in degree of freedom j to a disturbance in degree of freedom i. These coefficients are of the general form

$$K_{ij}^* = -\frac{\partial F_j^*}{\partial X_i^*} \tag{3}$$

and

$$D_{ij}^* = -\frac{\partial F_j^*}{\partial \dot{X}_i^*} \tag{4}$$

For small perturbation the dynamic coefficients are obtained by perturbing only one degree of freedom at a time while holding all others fixed at their equilibrium positions.

In order to evaluate the stiffness and damping coefficients the system of fluid film forces and moments acting on the seal ring has to be known. This system is the result of the fluid film pressure generated in the sealing gap by hydrostatic, hydrodynamic, and squeeze film effects. Hydrostatic and hydrodynamic effects were analyzed in [17] and [18], respectively. In both cases a general model of coned face seal having a coning β^* (see Fig. 2) was considered and the complete range of tilt parameter, ϵ, was covered. In [19] squeeze effect was analyzed for $\beta^* = 0$. From these works it is more convenient to obtain the fluid film moments about axes 1 and 2 of the rotating coordinate system 123. Hence, the angular stiffness and damping coefficients in this report will also be calculated with respect to the 123 system. The results can then be transformed to any other preferred system of coordinates.

Assuming that the fluid film in the sealing gap is complete namely, cavitation does not occur, it can be easily shown that the hydrodynamic pressure component is antisymmetric with respect to axis 2. Hence, the hydrodynamic effect contributes only a transverse moment M_2^* about axis 2. The hydrostatic and the squeeze film effects on the other hand generate, for the case of full fluid film, pressure components that are symmetric with respect to axis 2. Hence, these effects contribute only moments M_1^* about axis 1 and forces F_z^* along axis z. Using axis 3 instead of z to describe the axial degree of freedom (which is justified since γ^* is extremely small in any practical seal), we can conclude that in the rotating reference system 123 K_{11}^*, K_{33}^* and their cross coupled coefficients have only hydrostatic components, while K_{12}^*, K^*_{32} have only hydrodynamic components, also, all the damping coefficients D_{ij}^* where $j = 2$ vanish. Since no tilt is taking place about axis 2 all the coefficients K_{ij}^* and D_{ij}^* where $i = 2$ are identically zero.

Stiffness and Damping Coefficients

The expressions for axial forces and tilting moments generated by the hydrodynamic, hydrostatic, and squeeze effects are quite complex and cumbersome when the full range of the tilt parameter, ϵ, is considered. For small perturbation, however, when it can be assumed that $\epsilon^2 << 1$ these expressions can be much simplified. The simplified expressions for the forces and moments are presented in the following.

The hydrostatic components of the axial force and the tilting moment about axis 1 were found in [17]. Using the normalized expressions for all the relevant parameters the hydrostatic force has the form

$$(F_z)_s = \frac{\pi}{2}(1-R_i^2)(P_i+P_0) + \pi(P_0-P_i)\delta(1-R_i)E \tag{5}$$

where

$$E = \frac{(1-R_i)R_m}{2+\delta(1-R_i)} \tag{6}$$

The normalized hydrostatic moment is

Nomenclature

C = seal center-line clearance
C_0 = equilibrium center-line clearance
D_{ij}^* = damping coefficient
D_{ij} = normalized damping, equations (22), (23)
E = stiffness parameter, equation (6)
F_j^* = generalized force
F^* = force
F = normalized force, F^*/Sr_0^2
G = damping parameter, equation (9)
H = normalized film thickness, h/C
h = film thickess
K_{ij}^* = stiffness coefficient
K_{ij} = normalized stiffness, equations (20), (21)
M^* = moment
M = normalized moment, M^*/Sr_0^3
m_j^* = generalized mass
P = normalized pressure, p/S
p = pressure
R = normalized radius, r/r_0
r = radius
S = seal parameter, $6\mu\omega(r_0/C_0)^2(1-R_i)^2$
t^* = time
t = normalized time, ωt^*
Z^* = axial displacement
Z = normalized displacement, Z^*/C_0
β^* = coning angle
β = normalized coning, $\beta^* r_0/C_0$
γ^* = nutation
γ = normalized nutation, $\gamma^* r_0/C_0$
δ = coning parameter, $\beta^* r_0/C$
ϵ = tilt parameter, $\gamma^* r_0/C$
θ = angular coordinate
μ = viscosity
ψ^* = precession angle
$\dot{\psi}$ = normalized precession, $\dot{\psi}^*/\omega$
ω = shaft angular velocity

Subscripts

1, 2, 3 = axes 1, 2, or 3, respectively
i = inner radius
m = mid radius
0 = outer radius, or $Z = 0$
q = squeeze effect
s = hydrostatic effect
z = axis z

Table 1 Stiffness and damping coefficients, K_{ij} and D_{ij}

		$j=1$	$j=2$	$j=3$
$i=1$	K	$\pi(P_0-P_i)(\beta R_i-1)E_0^2$	$2\pi R_m^3 G_0\left(\dot{\psi}-\frac{1}{2}\right)$	0
	D	$2\pi R_m^3 G_0$	0	
$i=2$	K and D	0	0	0
$i=3$	K	0	0	$\pi(P_0-P_i)\frac{2\beta}{R_m}E_0^2$
	D			$4\pi R_m G_0$

$$E_0=\frac{(1-R_i)R_m}{2+\beta(1-R_i)}$$

$$G_0=\frac{\ln[1+\beta(1-R_i)]-2\dfrac{\beta(1-R_i)}{2+\beta(1-R_i)}}{\beta^3(1-R_i)^2}$$

$$G_{0_{\beta=0}}=\frac{1-R_i}{12}$$

$$(M_1)_s=\pi(P_0-P_i)E^2(1-\delta R_i)\epsilon \tag{7}$$

The hydrodynamic moment about axis 2 was found in [18] by tedious integration. It is rederived in the Appendix for the case of $\epsilon^2 << 1$ and has the form

$$M_2=\pi R_m^3(1-2\dot{\psi})G\gamma \tag{8}$$

where

$$G=\frac{\ln[1+\delta(1-R_i)]-2\dfrac{\delta(1-R_i)}{2+\delta(1-R_i)}}{\delta(1+Z)^3[\delta(1-R_i)]^2} \tag{9}$$

The squeeze film components of the axial force and the tilting moment about axis 1 are also derived in the Appendix for $\epsilon^2 << 1$. The normalized axial force has the form

$$(F_z)_q=-4\pi R_m G\dot{Z} \tag{10}$$

and the normalized moment is

$$(M_1)_q=-2\pi R_m^3 G\dot{\gamma} \tag{11}$$

In equations (5) through (11) δ is the coning parameter given by $\delta=\beta^* r_0/C$ where

$$C=C_0(1+Z) \tag{12}$$

Hence

$$\delta=\frac{\beta}{1+Z} \tag{13}$$

where β is the normalized coning defined as $\beta=\beta^* r_0/C_0$.

Recalling that for small perturbation the dynamic coefficients are obtained by perturbing only one degree of freedom at a time while holding all others fixed at their equilibrium positions, we can proceed and calculate the dynamic coefficients from the relevant forces and moments.

From equations (5) and (6) it is clear that $K_{13}=0$. The axial stiffness K_{33} is obtained from

$$K_{33}=-\frac{\partial(F_z)_s}{\partial Z}$$

Hence, using equation (13)

$$K_{33}=\pi(P_0-P_i)\frac{E_0^2}{R_m}2\beta \tag{14}$$

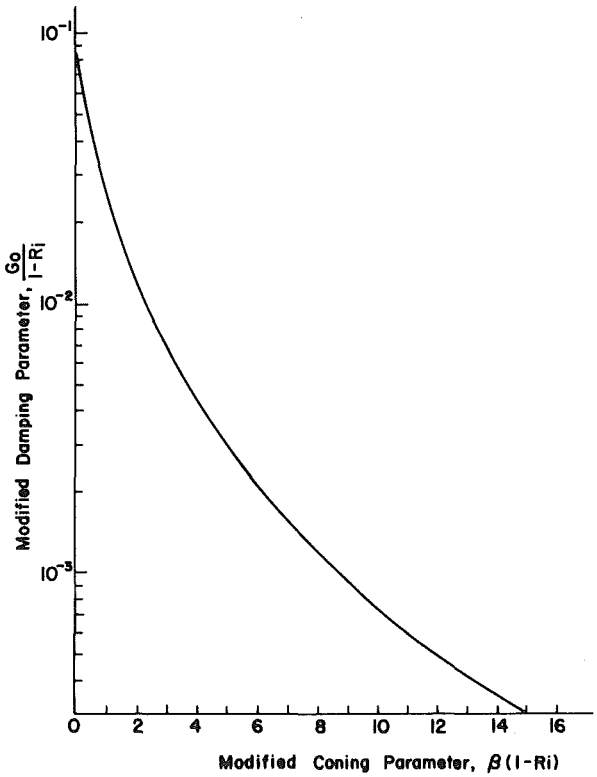

Fig. 3 Modified damping parameter as function of modified coning parameter

where E_0 is the corresponding value of E (see equation (6)) at equilibrium ($Z=0$).

The tilt parameter ϵ is given by $\epsilon=\gamma^* r_0/C$ hence,

$$\epsilon=\frac{\gamma}{1+Z} \tag{15}$$

Substituting equation (15) in (7) it is clear that $K_{31}=0$. The angular stiffness K_{11} is obtained from

$$K_{11}=-\frac{\partial(M_1)_s}{\partial\gamma}$$

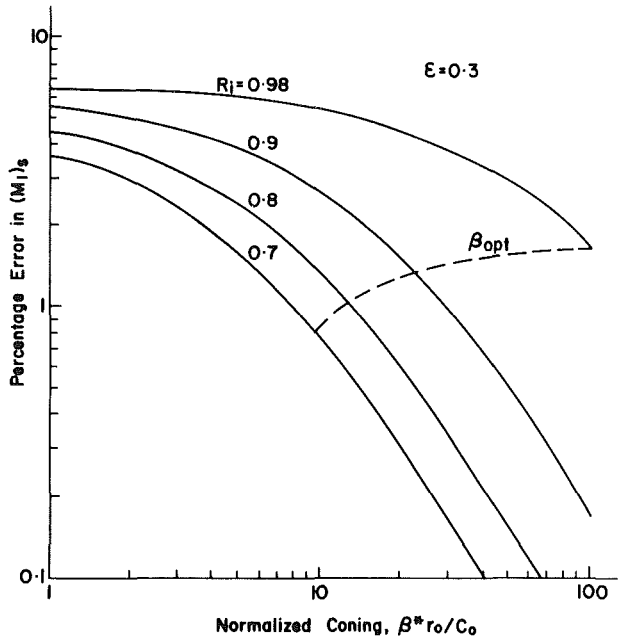

Fig. 4 Percentage error in the normalized hydrostatic moment, $(M_1)_S$, versus the normalized coning, β, for various radius ratios, R_i, at $\epsilon = 0.3$

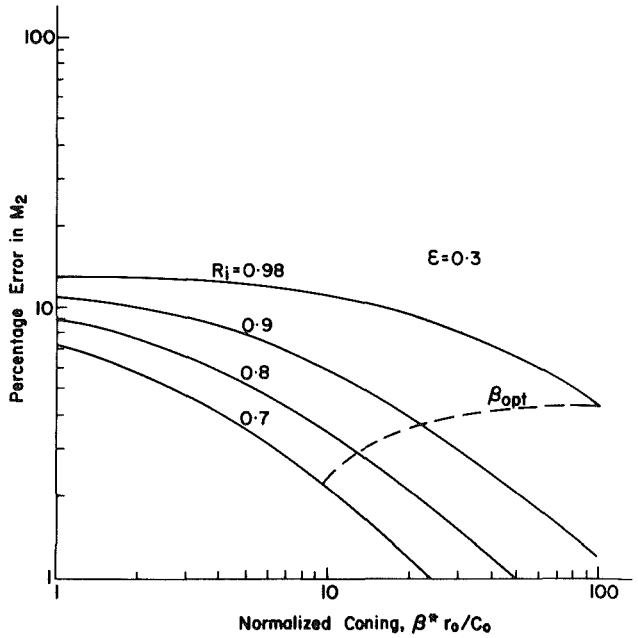

Fig. 5 Percentage error in the normalized hydrodynamic transverse moment, M_2, versus the normalized coning, β, for various radius ratios, R_i, at $\epsilon = 0.3$

Hence, by (15)

$$K_{11} = \pi(P - P_i)(\beta R_i - 1)E_0^2 \tag{16}$$

From equation (8) the normalized transverse stiffness coefficient K_{12} is

$$K_{12} = 2\pi R_m^3 G_0 \left(\dot{\psi} - \frac{1}{2}\right) \tag{17}$$

where G_0 is the corresponding value of G (see equation (9)) at equilibrium ($Z = 0$).

As can be seen from (17) the cross coupled stiffness K_{12} depends on the precession $\dot{\psi}$ and hence, is nonlinear. In many practical cases, when the seal ring tracks synchronously the motion of the rotating seat, the precession $\dot{\psi}^*$ is equal to the shaft speed ω. In these cases we have $\dot{\psi} = 1$ and K_{12} becomes linear. For a general nonsynchronous solution, however, the nonlinear expression for K_{12} as given in (17) has to be used.

From equations (10) and (11) the normalized damping coefficients are

$$D_{33} = 4\pi R_m G_0 \tag{18}$$

and

$$D_{11} = 2\pi R_m^3 G_0 \tag{19}$$

It is also clear that $D_{13} = D_{31} = 0$.

The normalized dynamic coefficients are related to the corresponding actual ones by the following normalization factors.

Axial stiffness by

$$K_{33} = \frac{K_{33}^*}{Sr_0}\frac{C_0}{r_0} \tag{20}$$

Angular stiffness by

$$K_{1j} = \frac{K_{1j}^*}{Sr_0}\frac{C_0}{r_0^3} \quad j = 1, 2 \tag{21}$$

Axial damping and angular damping by

$$D_{33} = \frac{D_{33}^*}{Sr_0}\frac{C_0}{r_0}\omega \tag{22}$$

and

$$D_{11} = \frac{D_{11}^*}{Sr_0^3}\frac{C_0}{r_0}\omega \tag{23}$$

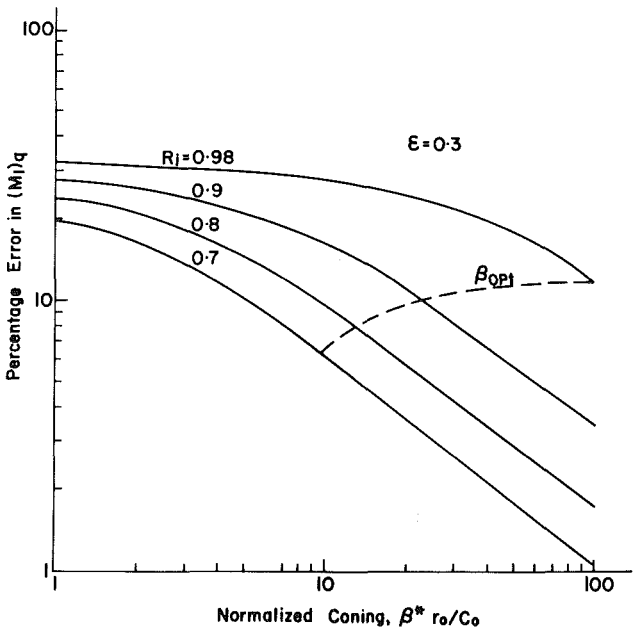

Fig. 6 Percentage error in the normalized squeeze moment, $(M_1)_q$, versus the normalized coning, β, for various radius ratios, R_i, at $\epsilon = 0.3$

By expanding G_0 as a series of $\beta(1 - R_i)$ it can be shown that in the limiting case $\beta = 0$, which corresponds to flat face seals, the function G_0 is

$$G_{0_{\beta=0}} = \frac{1 - R_i}{12} \tag{24}$$

Hence, all the dynamic coefficients presented here are also applicable for flat face seals where $\beta = 0$. The results for K_{ij} and D_{ij} are summarized in Table 1.

Discussion of the Results

The information provided in Table 1 can be used to calculate the various components of forces and moments according to equation (2) which can then be used in the

equations of motion (1). The substitution is straightforward and the system of fluid film forces and moments for small perturbation thus become

$$F_z = -K_{33}Z - D_{33}\dot{Z} \tag{25}$$

$$M_1 = -K_{11}\gamma - D_{11}\dot{\gamma} \tag{26a}$$

$$M_2 = -K_{12}\gamma \tag{26b}$$

As can be seen from Table 1 the various dynamic coefficients depend on the coning β via the parameters E_0 and G_0. Figure 3 presents the variation of G_0 versus $\beta(1-R_i)$. From the figure it is clear that the coning reduces G_0 and thus, reduces the axial and angular damping of the fluid film. Hence, from the point of view of damping, flat faces are preferable to coned faces.

Increasing the coning β reduces the effect of the cross coupled stiffness coefficient K_{12} and therefore reduces the transverse hydrodynamic moment M_2 of equation (26*b*). The moment M_2 is affected also by the precession $\dot{\psi}$ and, as can be seen from Table 1, at $\dot{\psi} = 0.5$ the transverse moment vanishes completely. From equation (29) of the Appendix the same effect can be seen on the hydrodynamic component of the pressure P. From equation (29) it is clear that the range of $0 < \dot{\psi} < 1$ corresponds to reduced hydrodynamic effect. Because of the flexible support of the ring $\dot{\psi}$ is normally in that range and hence, in practical seals the hydrodynamic effect may be less significant than the other effects. A small hydrodynamic effect makes the assumption of a complete fluid film without cavitation more valid. This is because cavitation is the result of hydrodynamic effect in diverging gaps.

The effect of coning on the axial and angular stiffness coefficients is very interesting. At $\beta = 0$ K_{33} vanishes and therefore flat face seals do not have any axial stiffness. Increasing the coning will increase both K_{11} and K_{33} up to a maximum after which a further increase in β will cause a drop in stiffness. Hence, there is an optimum coning for maximizing the stiffness of fluid film in face seals. By differentiating K_{11} and K_{33} of Table 1 with respect to β it can be easily shown that the optimum coning for K_{11} is

$$\beta_{\text{opt}} = \frac{2}{R_i(1-R_i)} \tag{27a}$$

while the optimum coning for K_{33} is

$$\beta_{\text{opt}} = \frac{2}{1-R_i} \tag{27b}$$

It is interesting to note that the optimum coning for angular stiffness is identical to the optimum coning that was found empirically in [7] for maximum dynamic stability. Since in practical seals R_i is close to unity there is not much difference between the optimum conings of equations (27*a*) and (27*b*) and either one can be used as a guide for maximum stiffness design.

Since the dynamic coefficients in Table 1 are based on small tilt namely, $\epsilon^2 << 1$, it may be of interest to know the range of tilt parameter values, ϵ, for which Table 1 is still applicable. For this purpose the various components of the axial force F_z and the moments M_1 and M_2 of equations (25) to (27) were compared with the corresponding values derived from more rigorous analyses, e.g. references [17], [18] and a numerical integration of equation (29) of the Appendix where the complete range of ϵ is covered. The results in terms of the percentage error are presented in Figs. 4 to 6. All the results are for the case $\epsilon = 0.3$ and show the percentage error versus coning parameter β at various values of the radius ratio R_i. The locus of the optimum coning for maximizing angular stiffness

$$\beta_{\text{opt}} = \frac{2}{R_i(1-R_i)}$$

is shown too. Figure 4 presents the results for the hydrostatic moment $(M_1)_s$, and Figs. 5 and 6 present the results for the hydrodynamic transverse moment M_2 and squeeze film moment $(M_1)_q$, respectively. In all three cases the percentage error decreases with increasing coning. The worst case is that of the squeeze film effect shown in Fig. 6 where the error can reach values as high as 32 percent at $R_i = 0.98$ and $\beta = 1$. For $\beta \geq \beta_{\text{opt}}$ and $R_i \leq 0.9$ the error at $\epsilon = 0.3$ is always less than 10 percent. The accuracy is much better when the hydrostatic component of M_1 is considered (see Fig. 4). Here the error is less than 7 percent for the complete range covered in the figure. The hydrodynamic transverse moment, M_2, can be calculated by using Table 1 within an accuracy of 10 percent or better for $R_i \leq 0.9$ up to $\epsilon = 0.3$. The percentage error in the axial force was found to be always smaller than that of the corresponding component of the moment and hence is not presented.

From the comparison discussed above it can be concluded that the results of Table 1 can be used safely up to $\epsilon = 0.3$ provided that $\beta \geq \beta_{\text{opt}}$ and that no cavitation occurs. For flat face seals where $\beta = 0$ the range of ϵ permitting the use of Table 1 for calculating forces and moments will be less than 0.3 mainly because of the error involved in the squeeze film effect.

Concluding Remarks

The dynamic coefficients of the fluid film in a mechanical face seal are calculated based on small perturbation of the seal ring. The seal model used is that of the coned face type, however, the results are applicable for flat face seals as well.

The effect of coning on the various dynamic coefficients is discussed, and optimization with respect to the axial and angular stiffness of the fluid film is pointed out.

The tabulated results of the dynamic coefficients can be used for small perturbation dynamic analyses of mechanical face seals. These results can also be used within an accuracy of 10 percent to calculate various fluid film forces and moments acting on the seal ring up to significant values of tilt of the ring with respect to its center line.

References

1 Metcalfe, R., "Dynamic Whirl in Well Aligned, Liquid Lubricated End Face Seals with Hydrostatic Tilt Instability," *ASLE Trans.*, Vol. 25, No. 1, Jan. 1982, pp. 1-6.

2 Rowles, R. T., and Nau, B. S., "An Assessment of Factors Affecting the Response of Mechanical Face Seals to Shaft Vibration," *Proc. 8th Int. Conf. on Fluid Sealing*, BHRA, Sept. 1978, paper A3.

3 Kittmer, C. A., and Metcalfe, R., "An Inside View of Rotary Seal Dynamics," *Proc. of the 5th Sym. on Engng. Applications of Mechanics*, Univ. of Ottawa, June 1980, pp. 201-208.

4 Nau, B. S., "Vibration and Rotary Mechanical Seals," *Tribology International*, Feb. 1981, pp. 55-59.

5 Etsion, I., and Dan, Y., "An Analysis of Mechanical Face Seal Vibrations," ASME JOURNAL OF LUBRICATION TECHNOLOGY, Vol. 103, No. 3, July 1981, pp. 428-435.

6 Metcalfe, R., "Dynamic Tracking of Angular Misalignment in Liquid Lubricated End-Face Seals," *ASLE Trans.*, Vol. 24, No. 4, Oct. 1981, pp. 509-516.

7 Etsion, I., "Dynamic Analysis of Noncontacting Face Seals," ASME JOURNAL OF LUBRICATION TECHNOLOGY, Vol. 104, No. 4, Oct. 1982, pp. 460-468.

8 Etsion, I., and Auer, B. M., "Simulation and Visualization of Face Seal Motion Stability by Means of Computer Generated Movies," 9th Int. Conference of Fluid Sealing, BHRA, 1981, paper E1.

9 Wu, Y. T., and Burton, R. A., "Thermoelastic and Dynamic Phenomena in Seals," ASME JOURNAL OF LUBRICATION TECHNOLOGY, Vol. 103, No. 2, Apr. 1981, pp. 253-260.

10 Matt, R. J., "High Temperature Metal Bellows Seals for Aircraft and Missile Accessories," ASME *Journal of Engineering for Industry*, Vol. 85, Aug. 1963, pp. 281-288.

11 Hudelson, J. C., "Dynamic Instability of Undamped Bellows Face Seals in Cryogenic Liquid," *ASLE Trans.*, Vol. 9, No. 4, Oct. 1966, pp. 381-390.

12 Storm, T. N., Ludwig, L. P., and Hudelson, J. C., "Vibration of Shaft Face Seals and Stabilizing Effect of Viscous and Friction Damping," NASA TN D-5161, Apr. 1969.

13 Kupperman, D. A., "Dynamic Tracking of Noncontacting Face Seals," *ASLE Trans.*, Vol. 18, No. 4, Oct. 1975, pp. 306-311.

14 Haardt, R., and Godet, M., "Axial Vibration of a Misaligned Radial Face Seal Under a Constant Closure Force," *ASLE Trans.*, Vol. 18, No. 1, Jan. 1975, pp. 56-61.
15 Griskin, E. N., "The Effect of Dynamics of Fluid Flow in a Face Seal," *Proc. 7th Int. Conf. on Fluid Sealing*, BHRA, Sept. 1975, paper B2.
16 Ludwig, L. P., and Allen, G. P., "Face Seal Lubrication II. Theory of Responses to Angular Misalignment," NASA TN D-8102, Mar. 1976.
17 Etsion, I., and Sharoni, A., "Performance of End Face Seals with Diametral Tilt and Coning - Hydrostatic Effects," *ASLE Trans.*, Vol. 23, No. 3, July 1980, pp. 279-288.
18 Sharoni, A., and Etsion, I., "Performance of End Face Seals with Diametral Tilt and Coning - Hydrodynamic Effects," *ASLE Trans.*, Vol. 24, No. 1, Jan. 1981, pp. 61-70.
19 Etsion, I., "Squeeze Effects in Radial Face Seals," ASME JOURNAL OF LUBRICATION TECHNOLOGY, Vol. 102, No. 2, Apr. 1980, pp. 145-152.

APPENDIX

Hydrodynamic and Squeeze Film Effects

The pressure distribution, p, in the sealing gap of a mechanical face seal can be found from a solution of the Reynolds equation which for practical narrow seals reduces to

$$\frac{\partial}{\partial r}\left(h^3\frac{\partial p}{\partial r}\right)=6\mu\left(\omega\frac{\partial h}{\partial\theta}+2\frac{\partial h}{\partial t^*}\right) \tag{28}$$

Due to its linear nature equation (28) can be solved separately for the hydrostatic, hydrodynamic, and squeeze components of the pressure [17-19]. The hydrodynamic and squeeze components can be combined yielding

$$p=-3\mu\left(\omega\frac{\partial h}{\partial\theta}+2\frac{\partial h}{\partial t^*}\right)\frac{(r_0-r)(r-r_i)}{h_m h^2}$$

or in a normalized form (see reference [7])

$$P=\left[\left(\frac{1}{2}-\dot{\psi}\right)\gamma R_m\sin\theta-(\dot{Z}+\dot{\gamma}R_m\cos\theta)\right]\frac{A}{(1+Z)^3}\,\frac{R-R_i}{1-R_i} \tag{29}$$

where

$$A=\frac{1-R}{H_m H^2(1-R_i)} \tag{30}$$

and

$$H=1+\epsilon R\cos\theta+\delta(R-R_i) \tag{31}$$

The system of forces and moments acting on the seal ring of Fig. 2 in the case of full fluid film (no cavitation) is

$$F_z=2R_m\int_0^\pi\int_{R_i}^1 P\,dR\,d\theta \tag{32}$$

$$M_1=2R_m^2\int_0^\pi\int_{R_i}^1 P\cos\theta\,dR\,d\theta \tag{33}$$

and

$$M_2=2R_m^2\int_0^\pi\int_{R_i}^1 P\sin\theta\,dR\,d\theta \tag{34}$$

From equations (29) through (34) it can be seen that a common integral $T(\theta)$ is required for evaluating the force and moments, where

$$T(\theta)=\int_{R_i}^1\frac{(1-R)(R-R_i)}{H_m H^2}\,dR$$

Evaluating $T(\theta)$ yields

$$T(\theta)=2\left[\frac{\ln H_0-\ln H_i}{(\delta+\epsilon\cos\theta)^3}-\frac{1-R_i}{H_m(\delta+\epsilon\cos\theta)^2}\right] \tag{35}$$

Rearranging equation (31) in the form

$$H=[1+\delta(R-R_i)][1+\alpha(R)\cos\theta] \tag{36}$$

where

$$\alpha(R)=\frac{\epsilon R}{1+\delta(R-R_i)}$$

we have for $\epsilon^2<<1$, and hence $\alpha^2<<1$,

$$\ln H=\alpha'(R)+\alpha(R)\cos\theta \tag{37}$$

where

$$\alpha'(R)=\ln[1+\delta(R-R_i)] \tag{38}$$

Substituting (38) into (35) and using the expansion

$$(1+\bar{\epsilon}\cos\theta)^{-n}=1-n\bar{\epsilon}\cos\theta$$

where $\bar{\epsilon}=\epsilon/\delta$ and $\bar{\epsilon}^2<<1$, we finally have

$$T(\theta)=\frac{2\alpha'(1)}{\delta^3}+\frac{2\cos\theta}{\delta^3}[\alpha(1)-\alpha(R_i)-3\alpha'(1)\bar{\epsilon}]$$

$$-\frac{2(1-R_i)}{\delta^2[1+\delta(R_m-R_i)]}+2(1-R_i)\frac{\cos\theta}{\delta^2}\,\frac{\alpha(R_m)+2\bar{\epsilon}}{1+\delta(R_m-R_i)} \tag{39}$$

Using equation (39) in the evaluation of the hydrodynamic and squeeze components of equations (32) to (34) we have

$$(F_z)_q=-\frac{2R_m}{(1+Z)^3(1-R_i)^2}\int_0^\pi(\dot{Z}+\dot{\gamma}R_m\cos\theta)\,T(\theta)\,d\theta \tag{40}$$

$$(M_1)_q=-\frac{2R_m^2}{(1+Z)^3(1-R_i)^2}\int_0^\pi(\dot{Z}+\dot{\gamma}R_m\cos\theta)\cos\theta T(\theta)\,d\theta \tag{41}$$

$$M_2=\frac{(1-2\dot{\psi})\gamma R_m^3}{(1+Z)^3(1-R_i)^2}\int_0^\pi\sin^2\theta T(\theta)\,d\theta \tag{42}$$

Neglecting second order terms such as $\dot{Z}\epsilon$, $\dot{\gamma}\alpha(R)$ etc. since we are interested in small perturbation only, the integrations of equations (40) to (42) result in

$$(F_z)_q=-4\pi R_m G\dot{Z} \tag{43}$$

$$(M_1)_q=-2\pi R_m^3 G\gamma \tag{44}$$

and

$$M_2=\pi R_m^3(1-2\dot{\psi})G\gamma \tag{45}$$

where

$$G=\frac{\ln[1+\delta(1-R_i)]-2\dfrac{\delta(1-R_i)}{2+\delta(1-R_i)}}{\delta(1+Z)^3[\delta(1-R_i)]^2}$$